The molecular mechanism of lipid monolayer collapse

Baoukina, Svetlana; Monticelli, Luca; Risselada, H. Jelger; Marrink, Siewert J.; Tieleman, D. Peter

Published in:
Proceedings of the National Academy of Sciences of the United States of America

DOI:
10.1073/pnas.0711563105

Publication date:
2008

Supporting Information

Baoukina et al. 10.1073/pnas.0711563105

SI Text

Materials. ***Structural and dynamic characteristics of monolayers near collapse.*** The monolayer surface tension as function of area per lipid for both compositions (DPPC and POPG in ratios of 4:1 and 1:1) at 310 K is shown in Fig. 2*a*. The monolayers remain in a flat geometry at the interface at positive surface tensions, whereas at negative surface tensions, they become unstable and collapse. At near-zero surface tensions before collapse the monolayers of both compositions form a homogeneous liquid-expanded phase. At the surface tension of $\gamma_m \approx 1$ mN/m, the average areas per lipid, A_L, are 0.551 and 0.557 nm^2 in the 4:1 and 1:1 mixtures, respectively. The orientational order parameters $S_z = \langle 1/2(3\cdot\cos^2\theta - 1)\rangle$ (where θ is the angle with the monolayer normal) for the bonds between the coarse-grained particles constituting the DPPC and POPG lipids are shown in Fig. S1. Although the hydrocarbon chains are partially ordered because of close packing of molecules in the monolayer, the order parameters are significantly lower than in the liquid-condensed phase (1). The radial distribution functions (see Fig. S1) show that there is no long-range translational order or any demixing of lipid components. The coefficients of (long-time) lateral diffusion of lipids are $(2.7 \pm 0.2)\cdot 10^{-7}$cm^2/s and $(2.5 \pm 0.3)\cdot 10^{-7}$cm^2/s for the 4:1 and 1:1 mixtures, respectively, typical of a liquid phase (2, 3).

"Nucleation" of folds upon monolayer collapse. It has been shown theoretically (4) that folding of a monolayer is mathematically analogous to the formation of a crack in an elastic plate (5). At the surface of the crack, the stress induced by the crack equals the external load. At the monolayer–bilayer fold connection, the fold-induced stress (in the monolayer plane) equals the difference between the energy density of fold formation, ε, pulling material into the fold, and the monolayer surface tension, γ_m, pulling material out of the fold. The boundary conditions for the crack and the fold have the same mathematical form. Similar to the critical crack size, the critical fold length, L_c^{cr} (i.e., above which the fold will grow) is determined by the competition of its tendency to grow due to stress divergence at the endpoints and to shrink due to a line tension, λ_c, at the fold connection to the monolayer and is given by $L_c^{cr} = 2\lambda_c Y/(\pi(\epsilon - \gamma_m)^2)$, where ε is the energy density of fold formation, which can be estimated (4) as the surface tension of the hydrocarbon chain–water interface (≈22–25 mN/m); Y is the two-dimensional Young modulus of the monolayer: $Y = 4\cdot K_A\cdot G/(K_A + G)$, where K_A and G are area compression and shear moduli, respectively. The energy barrier for fold nucleation equals $\Delta E = 1/2\cdot\lambda_c\cdot L_c^{cr}$. The fold shape can be described by using the formula for the shape of the crack (4): $D(x)/L_c = (\varepsilon - \gamma_m)/Y\sqrt{1 - (2x/L_c)^2}$, where $D(x)$ is fold depth, L_c is the length of the fold connection to the monolayer, x is the coordinate along the fold connection (see Fig. S2). Based on the above equation, the bilayer folds connected to the monolayer have a semielliptical shape. For a viscoelastic monolayer, it describes the shape of the fold at short times (compared with the relaxation time), whereas at long times, it describes the flow profile (4). The transfer of the material from the monolayer into the fold is stopped as the compression is stopped, and the surface tension in the monolayer, γ_m, reaches the equilibrium value.

Transformations of folds and equilibrium structure. Bilayer folds connected to the monolayer change their shape with time and can transform into a vesicle and detach from the monolayer. These transformations depend on several macroscopic properties. To explain this dependence, we consider the following idealized shapes: (*i*) a semicircular bilayer fold connected to a monolayer; (*ii*) a separate flat circular bilayer in water; (*iii*) a semivesicle connected to a monolayer; (*iv*) a separate vesicle in water. Here, we assume that the amount of lipids in the collapsed aggregate does not change as the monolayer maintains the equilibrium tension. For simplicity, we also assume that the line tensions do not change with curvature along the bilayer perimeter and along the monolayer–bilayer connection. We also neglect the vesicle spontaneous curvature (associated, e.g., with different numbers of lipids in the leaflets) and the contributions from area stretching deformations. The energy of a flat bilayer of radius R in water is associated with its open edges and equals: $2\pi\cdot\lambda_p\cdot R$, where λ_p is the line tension at the bilayer perimeter. The energy of a semicircular bilayer fold of radius R connected to the monolayer also includes the contribution from the line tension, λ_c at the monolayer–bilayer connection: $\pi\cdot\lambda_p\cdot R + 2R\lambda_c$. The bending energy to create a spherical vesicle can be estimated according to the curvature elasticity model (6) as $1/2\cdot K_b\cdot(2/R)^2\cdot 4\pi\cdot R^2 = 8\pi\cdot K_b$ and is independent of its radius. The energy of a semivesicle connected to the monolayer equals $4\pi\cdot K_b + 2\pi\cdot\lambda_c\cdot R$.

To characterize the tendency of a flat bilayer to separate from the monolayer, we compare the energies of s semicircular fold (of radius R_1) connected to the monolayer and a separate circular bilayer (of radius $R_2 = R_1/\sqrt{2}$). The connected bilayer is more favorable if the following ratio for the line tensions at the monolayer–bilayer connection (λ_c) and at the bilayer perimeter (λ_p) holds: $\lambda_c/\lambda_p < \pi(\sqrt{2} - 1)/2 \approx 2/3$. Then, a flat semicircular bilayer fold of radius R_1 will form a semivesicle (of radius $R_3 = R_1/2$) connected to the monolayer if: $R_1 > 4K_b/(\lambda_p - (1 - 2/\pi)\lambda_c) \approx 4K_b/(\lambda_p - 1/3\lambda_c)$. A semivesicle of radius R_3 will detach from the monolayer to form a vesicle (of radius $R_4 = R_3/\sqrt{2}$) if $R_3 > 2K_b/\lambda_c$. Finally, a separate flat circular bilayer of radius R_2 will transform into a vesicle (of radius $R_4 = R_2/2$) if $R_2 > 4K_b/\lambda_p$.

Although a more detailed analysis (for example, including the vesicle spontaneous curvature or considering more complex shapes) could be performed, the outlined simple arguments are sufficient to explain the trends in the transformations of lipid aggregates.

Combining the calculated values with the above formulas, we obtain the following estimates. In the 1:1 mixture, the fold will remain connected to the monolayer maintaining a semicircular (or semielliptic) shape; it will transform into a semivesicle for $R_1 > 13$ nm, which is favorable to detach from the monolayer for $R_1 = 2R_3 > 36$ nm. In the 4:1 mixture, separation of the flat semicircular folds from the monolayer is also not favorable. The flat semicircular fold will transform into a semivesicle only for $R_1 > 23$ nm, which will detach from the monolayer if $R_1 = 2R_3 > 27$ nm. In the simulations, the bilayer folds initially have the radius of $R_1 \approx 16$ nm. In the 1:1 mixture, the above estimates are consistent with the simulation results, where the bilayer folds transform into semivesicles and remain connected to the monolayer. In the 4:1 mixture, the actual fold and vesicle shapes in the simulations (see Fig. 4 and Fig. S2) deviate from the considered idealized shapes.

Supplementary Methods. ***Calculation of the surface tension minus area isotherms.*** To calculate the surface tension minus area isotherms, we obtained a set of structures from the compression runs (with method 2 at the rate of −0.0308 nm/ns) of the large monolayers at different areas per molecule and performed simulations at constant volume, with constant monolayer area and fixed box size normal to the monolayers. From these simulations, the monolayer surface tension, γ_m, was calculated at each selected

area per lipid, A_L. The monolayer area compression moduli, K_A, were calculated from the slope of the tension-area isotherm using the formula: $K_A = A_L \cdot \partial\gamma_m/\partial A_L$.

For the mixture of DPPC and POPG in a ratio of 4:1, the simulated system contained 3,072 DPPC and 1,024 POPG lipids in each of the two monolayers and 317,277 water particles and 2,048 Na^+ ions in the box. For the mixture of DPPC and POPG in a ratio of 1:1, it contained 2,048 DPPC and 2,048 POPG lipids in each monolayer and 313,708 water particles and 4,096 Na^+ ions in the box. No pressure coupling was used. The simulation time was 400 ns per simulation.

Calculation of the monolayer shear moduli. To estimate the monolayer shear modulus as function of shear rate, we used a system with two smaller monolayers under dynamic shear deformation of the simulation box. The monolayer plane is parallel to the *xy* plane, and a continuous deformation is introduced in the *y* direction with the gradient in *x* direction at shear rates in the range $s \approx 0.2–0.001\ ns^{-1}$. The shear modulus, G, at a given shear rate, s, is calculated from the empirical rule relating the apparent shear viscosity and the complex viscosity (7) by using the following formula: $G(s) = (P_{xy}(s) \cdot L_z - \eta_w \cdot s \cdot L_w)/2$, where P_{xy} is the average stress in the box induced by the shear, 2 in the denominator accounts for two monolayers in the box, η_w is water viscosity, and L_w is the thickness of the water slab. The second term on the right-hand side represents the water contribution. The water viscosity, η_w, was calculated from independent simulations with two different methods: by introducing a dynamic shear deformation of the box and a periodic acceleration profile (8). Both methods provided the water viscosity of $(7.7 \pm 0.4) \cdot 10^{-4}$ Pa·s, independent of shear rate and in good agreement with the experimental value of $7 \cdot 10^{-4}$ Pa·s at 310 K (9).

The system setup included a water slab in vacuum with two symmetric monolayers at the two vacuum–water interfaces. For the mixture of DPPC and POPG in a ratio of 4:1, it contained 108 DPPC and 36 POPG lipids in each of the two monolayers and 3,928 water particles and 72 Na^+ ions in the box. For the mixture of DPPC and POPG in a ratio of 1:1, it contained 72 DPPC and 72 POPG lipids in each of the two monolayers and 3,856 water particles and 144 Na^+ ions in the box. For calculations of water viscosity, a water cube of size $10 \times 10 \times 10\ nm^3$, containing 8,312 water particles, was used. Before applying shear deformations, the systems were equilibrated for 400 ns at 310 K. The monolayers were simulated at the surface tension of 1 mN/m by using surface-tension coupling with compressibility of $5 \cdot 10^{-5}\ bar^{-1}$ in the lateral direction and zero in the normal direction, which provided fixed normal size of the box. The water cube was simulated at the bulk pressure of 1 bar by using the isotropic pressure-coupling scheme. Under dynamic deformations, no pressure coupling was used. The production runs were 4-μs long for the systems with the monolayers and 800-ns to 4-μs long for the water cube depending on the shear rate and the method.

Calculation of the bending modulus. To calculate the bending modulus of a lipid bilayer, we simulated a cylindrical bilayer in water (Fig. S3*c*). The cylinder axis was oriented along the *z* axis and the cylinder was periodic in the z direction. The bending modulus, K_b, is found from the tensile force, F_z, exerted by the cylinder in the *z* direction by using a simple formula (10): $K_b = (F_z \cdot R)/2\pi$, where R is the cylinder radius. The tensile force is calculated from the pressure tensor components using the following relation:

$F_z = (P_{zz} - P_b) \cdot A_{xy} + P_b \cdot A_c$, where $P_b = P_{xx} = P_{yy}$ is the pressure in the bulk water, A_{xy} is the box *xy*-area, and A_c is the cross-section area of the cylinder parallel to the xy-plane.

The starting structure for the cylinder was obtained by simulating self-assembly of lipids in a periodic box under cylindrically shaped harmonic restraints (11). The repulsive forces with a constant of 100 $kJ/mol \cdot nm^2$ were applied to restrain the lipids in a cylindrical shell with a radius of 10 nm. The relation between the cylinder radius and length and the required number of lipids was estimated by using the known area per lipid in a normal bilayer. Once a cylinder was formed, the restraints were removed. To ensure the cylinder is fully equilibrated, two artificial hydrophilic pores were introduced in cylinder walls in the radial direction. To this end, cylindrical restraints with a radius of 1.5 nm and a force constant of 50 $kJ/mol \cdot nm^2$ were applied on the hydrocarbon tails of the lipids. This allows fast solvent flux and flip–flop events between the inner and outer leaflets of the cylindrical bilayer. The restraints were released once the flip–flop rates between the two leaflets were equal and no net flux of solvent was observed.

For the DPPC and POPG 4:1 mixture, the bilayer cylinder contained 1,610 DPPC and 402 POPG lipids, with 52,917 water particles and 402 Na^+ in the box. For the 1:1 mixture, the bilayer contained 1,006 DPPC and 1,006 POPG lipids, with 48,538 water particles and 1,006 Na^+ in the box. The semiisotropic coupling scheme (with lateral pressure of 1 bar and zero compressibility in the normal direction) was used in all of the simulations of bilayer cylinders. The simulations included 400 ns of bilayer cylinder self-assembly with restraints, followed by 2 μs of production runs.

Calculation of the bilayer area compression modulus. Bilayer bending at high curvatures is coupled to area stretching deformations. To compare the contributions of the area stretching for the two mixtures (DPPC and POPG in ratios of 4:1 and 1:1), we also calculated the area compression moduli, K_A, at 310 K. To this end, we simulated small bilayers at various surface tensions. The obtained values are almost the same for both systems: $K_A = 220 \pm 30$ mN/m for the 4:1 mixture, and $K_A = 240 \pm 30$ mN/m for the 1:1 mixture. The calculated values are in good agreement with reported experimental (12) and simulation (13, 14) data. The length and unsaturation of the hydrocarbon chains do not significantly affect the area compression modulus. We thus expect that the area stretching gives a similar contribution to bending deformations (of similar magnitude) in both systems.

To calculate the bilayer area compression modulus, we simulated small bilayers in water under various surface tensions. The intrinsic (14) area compression modulus, K_A, is calculated from the slope of the tension-area dependence: $K_A = A_0 \cdot \partial\gamma/\partial A$, where A_0 is the equilibrium area of the (tensionless) bilayer.

For the 4:1 mixture, the bilayer contained 96 DPPC and 32 POPG with 2,291 water particles and 32 Na^+ ions. For the 1:1 mixture, the bilayer contained 64 DPPC and 64 POPG with 2,167 water particles and 64 Na^+ ions. Surface-tension coupling was used with compressibility of $5 \cdot 10^{-5}\ bar^{-1}$ in the normal and lateral directions; normal pressure was set to 1 bar. The surface tensions were set to 0, 50, 100, 200, and 300 bar·nm, corresponding to 0, 5, 10, 20 and 30 mN/m. The small bilayers were simulated for 4 μs each.

Calculation of the line tension. To calculate the line tension at the bilayer edge, we used the following setup. A bilayer slab was placed in a box of water so that it was surrounded by water in the *y* and *z* directions and was periodic in the *x* direction (Fig. S3*b*). The line tension at the bilayer edge, λ_p, is then found by using a simple formula (15): $\lambda_p = L_y \cdot L_z \cdot (P_b - P_{xx})/2$, where $P_b = P_{yy} = P_{zz}$ is the pressure in the bulk water, P_{xx} is the pressure tensor component along the bilayer edge, and L_y and L_z are box sizes in *y* and *z* directions, respectively.

For the 4:1 mixture, the bilayer contained 216 DPPC and 72 POPG with 7,946 water particles and 72 ions in the box. For the 1:1 mixture, the bilayer contained 144 DPPC and 144 POPG with 7,683 water particles and 144 ions in the box. Anisotropic pressure coupling was used, with *yy* and *zz* components of the

pressure tensor set to 1 bar (with compressibility of $5 \cdot 10^{-5}$ bar^{-1}); all of the other components of the compressibility tensor were set to zero. The bilayer slabs were simulated for 4 μs each.

To calculate the line tension at the bilayer-monolayer connection, the following setup was used. Two symmetric monolayers were placed at the two water–vacuum interfaces of a water slab; the monolayers were connected by a perpendicularly oriented (tensionless) bilayer through the water slab (Fig. S3*d*). If the bilayer lies in the *yz* plane, and the monolayers lie in the *xy* plane, then the line tension at the monolayer–bilayer connections, λ_c, can be estimated by using the following formula: $\lambda_c = L_x \cdot L_z \cdot (P_{xx} - P_{yy})/2$.

For the 4:1 mixture, the systems contained 432 DPPC and 144 POPG lipids, 4,275 water particles and 144 ions, whereas for the 1:1 mixture, 288 DPPC and 288 POPG lipids were used, with 4,056 water particles and 288 ions. The monolayer–bilayer setup was simulated at constant volume of the box for 4 μs for each composition.

1. Baoukina S, Monticelli L, Marrink SJ, Tieleman DP (2007) Pressure-area isotherm of a lipid monolayer from molecular dynamics simulations. *Langmuir* 23:12617–12623.
2. Almeida PFF, Vaz WLC, Thompson TE (1992) Lateral diffusion in the liquid-phases of dimyristoylphosphatidylcholine cholesterol lipid bilayers—A free-volume analysis. *Biochemistry* 31:6739–6747.
3. Tanaka K, Manning PA, Lau VK, Yu H (1999) Lipid lateral diffusion in dilauroylphosphatidylcholine/cholesterol mixed monolayers at the air/water interface. *Langmuir* 15:600–606.
4. Lu WX, Knobler CM, Bruinsma RF, Twardos M, Dennin M (2002) Folding Langmuir monolayers. *Phys Rev Lett* 89:146107.
5. Landau LD, Lifshitz EM (1980) *Theory of Elasticity* (Pergamon, New York).
6. Helfrich W (1973) Elastic properties of lipid bilayers: Theory and possible experiments. *Z Naturforsch C* 28:693–703.
7. Cox WP, Mertz EH (1958) Correlation of dynamic and steady flow viscosities. *J Polym Sci* 28:619–622.
8. Hess B (2002) Determining the shear viscosity of model liquids from molecular dynamics simulations. *J Chem Phys* 116:209–217.
9. Aleksandrov AA, Trakhtengerts MS (1974) Viscosity of water at temperatures of −20 to 150°C. *J Eng Phys* 27:1235–1239.
10. Harmandaris VA, Deserno M (2006) A novel method for measuring the bending rigidity of model lipid membranes by simulating tethers. *J Chem Phys* 125:204905.
11. Risselada HJ, Mark AE, Marrink SJ (2008) The application of mean field boundary potentials in simulation of lipid vesicles. *J Phys Chem B* 112:7438–7447.
12. Rawicz W, Olbrich KC, McIntosh T, Needham D, Evans E (2000) Effect of chain length and unsaturation on elasticity of lipid bilayers. *Biophys J* 79:328–339.
13. Marrink SJ, de Vries AH, Mark AE (2004) Coarse grained model for semiquantitative lipid simulations. *J Phys Chem B* 108:750–760.
14. Lindahl E, Edholm O (2000) Spatial and energetic-entropic decomposition of surface tension in lipid bilayers from molecular dynamics simulations. *J Chem Phys* 113:3882–3893.
15. Tolpekina TV, den Otter WK, Briels WJ (2004) Simulations of stable pores in membranes: system size dependence and line tension. *J Chem Phys* 121:8014–8020.

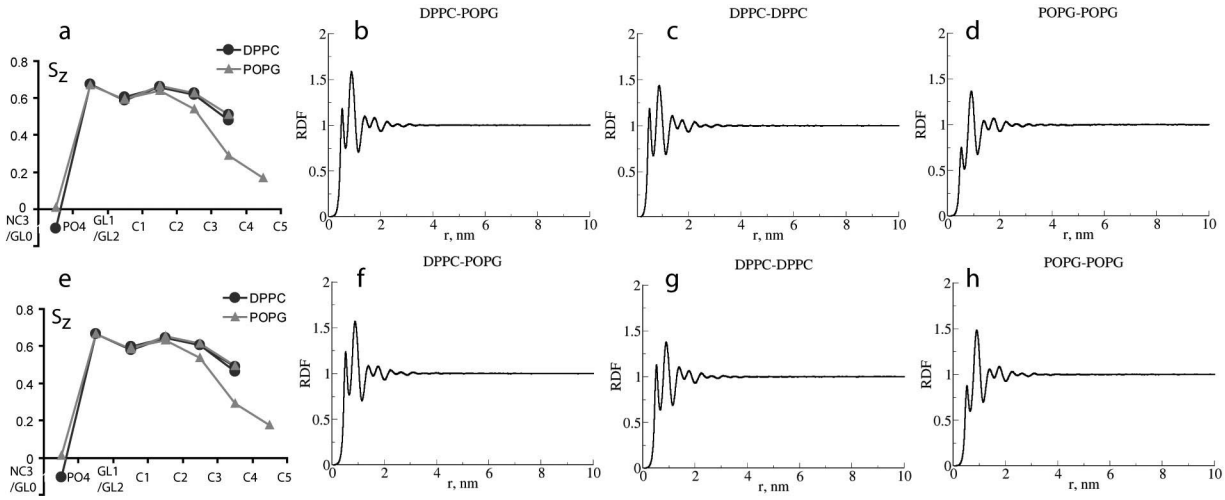

Fig. S1. Structural characteristics of lipid monolayers containing DPPC and POPG lipids in ratios of 4:1 (*a*–*d*) and 1:1 (*e*–*h*) at 310 K near collapse (at the surface tension ≈1 mN/m). Orientational order parameters for the bonds connecting the coarse-grained particles (including head group and two hydrocarbon chains) in DPPC and POPG lipids (*a* and *e*) and radial distribution function (*b*–*d* and *f*–*h*) of the phosphate centers of the lipids in the two mixtures are shown.

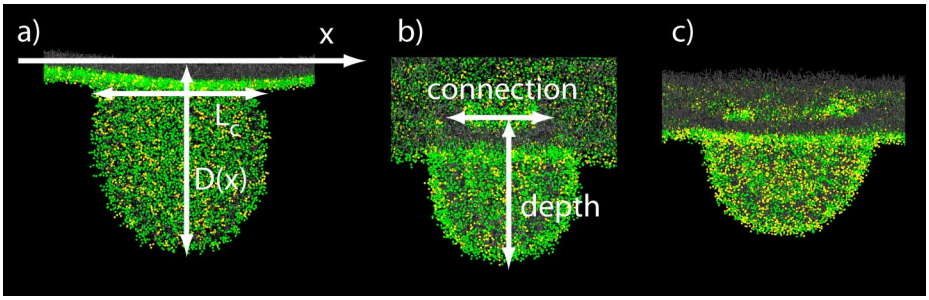

Fig. S2. Geometrical characteristics of the folds and vesicles formed in the DPPC:POPG 4:1 (*a*) and 1:1 (*b*) mixtures at 310 K. Color scheme is as in Fig. 4.

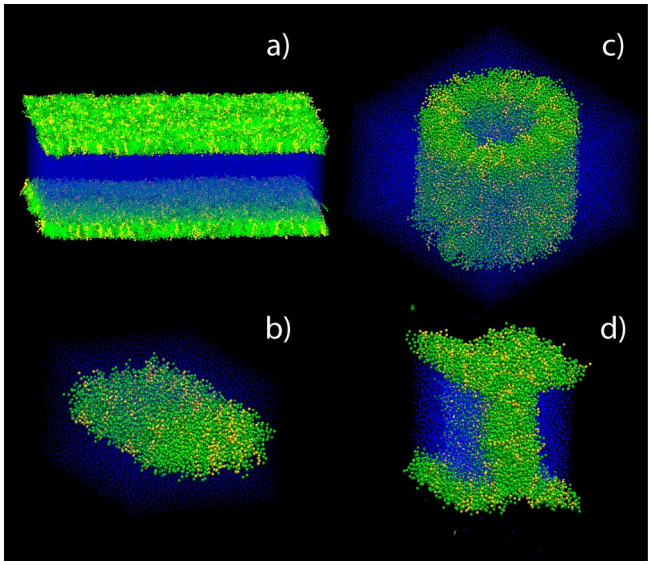

Fig. S3. The setup of the auxiliary simulations. (*a*) Two symmetric monolayers at the two water–vacuum interfaces to calculate the monolayer surface tension minus area isotherms, area compression and shear moduli; (*b*) A bilayer cylinder in water to calculate the bilayer bending modulus. (*c*) A bilayer slab in water to calculate line tension at the fold perimeter. (*d*) Two monolayers connected by a bilayer through water to calculate line tension at the connection of bilayer fold to monolayer. DPPC is shown in green, POPG in yellow, water in blue, and ions in gray.